

Comparison between the ROI based and pixel based analysis for neuroreceptor studies performed on the high resolution research tomograph (HRRT)

Vesna Sossi, *Member IEEE*, Stephan Blinder, Katherine Dinelle, Sarah Lidstone, Kevin J-C Cheng, Arman Rahmim, *Member, IEEE*, Siobhan McCormick, Doris J. Doudet, Thomas J. Ruth

Abstract—Parametric imaging refers to evaluating kinetic model parameters from time activity curves (TACs) estimated from every image pixel in contrast to region of interest (ROI) based analysis where the parameters are evaluated from TACs derived from predefined ROIs. Parametric imaging is thus more sensitive to statistical and motion induced noise. Here we evaluate the feasibility of parametric imaging for two modeling approaches, the simplified reference tissue model (RTM) and the tissue input Logan graphical method (L), for data acquired on the high resolution research tomograph (HRRT). The small image pixel size of this tomograph makes the image pixel values particularly sensitive to statistical noise and to artifacts due to subject motion. Comparing parametric BP estimates to those obtained with the ROI based approach a large downward bias (up to 28%) was observed for the Logan approach, while no bias was observed for the RTM method. The correlation between the BP values obtained with the ROI and parametric approach was better and less affected by motion for RTM ($r^2 > 0.9$) compared to L ($r^2 > 0.45$). The correlation between the BP obtained with the two methods was found to be significantly affected by patient motion and in general better for the ROI based approach. We conclude that parametric imaging on the HRRT is feasible for selected modeling approaches.

I. INTRODUCTION

KINETIC modeling is often used to reduce the temporal information obtained with dynamic positron emission tomography (PET) scanning into a few parameters related to the biological processes under investigation. For tracers that

bind in a reversible fashion two very commonly used approaches are the tissue input graphical Logan method (L) (1) and the simplified reference tissue (RTM) method (2,3). They both rely on similar assumptions, i.e. the existence of a reference region with negligible specific binding and the ratio k_1/k_2 (influx and efflux rate constant, respectively) not changing between the target region, which contains the specific binding sites, and the reference region, characterized by minimal or no specific binding. The L method makes no assumptions on the number of compartments, but it requires steady state between compartments to be reached during the course of the study. Two parameters are estimated with this approach, the distribution volume ratio (DVR), as the slope of the linear part of the Logan plot, and the intercept. The binding potential (BP) is derived from the DVR as $DVR-1$. The RTM requires the tracer kinetics in the target region to follow the one tissue compartment behavior and it estimates three parameters: BP, $R_1 = k_1/k_1'$ where k_1 and k_1' are the influx rate constants for the target and reference region respectively. The fact that the RTM method estimates one more parameter compared to the L approach makes it potentially intrinsically more sensitive to noise. The L method on the other hand is known to introduce a bias in the BP estimate, which depends on the BP magnitude itself and on the noise in the data (4).

Both methods lend themselves to parametric imaging, where BP is calculated using the time activity curves (TACs) obtained from each image pixel. In both cases the input function is generally derived from a TAC obtained from a region of interest (ROI) placed on the reference region. In the ROI based approach the BP is calculated using TACs of predefined target regions, which implies the need to pre-select regions and averaging over several pixel values. The advantage of the parametric approach is the fact that there is no need to predefine ROIs for which the BP is to be evaluated; this approach thus lends itself well to exploratory and comparative investigations where differences between studies are hypothesized but not necessarily spatially well defined. A potential drawback of the parametric approach is the fact that it is more sensitive to statistical noise in the data and to patient motion.

V.Sossi, K. Dinelle, K. J-C. Cheng, S. Lidstone and D. Doudet are with the University of British Columbia (UBC), Vancouver, B.C. V6T 1Z1, Canada, (e-mail vesna@phas.ubc.ca, kdinelle@phas.ubc.ca, jcheng@phas.ubc.ca., lidstone@interchange.ubc.ca)

S. Blinder and S. McCormick are with the Pacific Parkinson's Research Centre, Vancouver, BC, V6T 1Z1 (e-mail blinder@phas.ubc.ca, siobhan@pet.ubc.ca).

A. Rahmim was with the University of British Columbia, Vancouver, BC V6T 1Z1. He is now with the Department of Radiology, Johns Hopkins University School of Medicine, Baltimore, MD 21205 (e-mail arahmim1@jhmi.edu).

T. Ruth is with the TRIUMF, Vancouver B.C. V6T 1Z1 (e-mail truth@triumf.ca)

This work was supported by the Canadian Institute of Health Research, the TRIUMF Life Science grant, the Natural Sciences and Engineering Research Council of Canada UFA (V. Sossi), and the Michael Smith Foundation for Health Research scholarship (V. Sossi).

This problem might be exacerbated for high resolution scanners, such as the high resolution tomograph (HRRT) (5), which has a resolution of approximately $(2.5\text{mm})^3$. Although the sensitivity of this scanner is relatively high ($\sim 6\%$), the image pixel size ($1.22 \times 1.22\text{mm}^2$) is small; individual pixel values are likely to suffer significantly from statistical noise. In spite of these potential drawbacks dynamic images from this scanner are ideally suited to a parametric approach; the wealth of spatial information provided by this scanner (axial field of view 25 cm leading to a total of 207 1.2 mm thick imaging planes) makes it ideally suited for exploratory studies. These considerations provided the motivation for this study where we evaluate the feasibility of using parametric imaging on the HRRT for the RTM and Logan approach. Particular emphasis was placed on the effect of patient motion and patient motion correction (see the Methods section for additional considerations) on the accuracy of parametrically evaluated BP.

II. METHODS

A. Modeling approaches

The Logan graphical approach calculates the BP from the slope of the Logan plot as $\text{DVR} - 1$, as described in eq. 1.

$$\int_0^T C_T(t)dt / C_T(T) = \text{DVR} \left[\int_0^T C_R(t)dt + C_R(T)/k_2' \right] / C_T(T) + \text{int} \quad \text{eq. (1)}$$

where $C_T(t)$ is the radioactivity concentration in the target region, $C_R(t)$ is the radioactivity concentration in the reference region, int is the intercept term, which becomes a constant after a time t such that steady state between compartments has been reached. The RTM method obtains the parameters using equation 2:

$$C_T(t) = R_T C_R(t) + \{k_2 - R_T k_2' / (1 + \text{BP})\} C_R(t) \otimes \exp(-[k_2' / (1 + \text{BP})]t) \quad \text{eq. (2)}$$

where \otimes indicates the mathematical operation of convolution. The BP obtained with the Logan method will be denoted as BP_L and that obtained with the RTM method will be denoted BP_{RTM} .

B. Subjects and scans

Data from four human subjects were used for this study; two subjects (S1 and S2) were relatively still during the scanning session (movement < 3 mm in any direction) and two subjects (S3 and S4) experienced a considerable amount of motion (> 10 mm). The motion was monitored with the Polaris motion tracking system (6) throughout the duration of the scan (7). Fig 1 shows the motion associated with S3 where up to a 20 mm displacement was observed in the direction along the scanner axis (z-direction). After a 6 min transmission scan, the subjects were injected with 10 mCi of ^{11}C -raclopride

(RAC – a D2 receptor antagonist) and scanned for 60 min. Data were acquired in list mode and binned into 16 frames (4x1min, 3x2min, 8x5min, 1x10 min). Ordinary Poisson 3D-OSEM was used for reconstruction (8).

C. Motion correction

No online motion correction was performed, since an online motion correction algorithm was not available. An approximation to motion correction was performed by realigning the dynamic frames using a mutual information registration algorithm. This approach clearly under-corrects for motion, since it does not correct for motion within a frame; as a consequence an online motion correction method is expected to even further decrease the effects of motion in the case where motion was found to have a significant effect. Data obtained from the analysis of the realigned frames will be denoted as realigned (R), while those obtained from the non realigned frames will be referred to as non-realigned (NR). No realignment was performed between emission and transmission data.

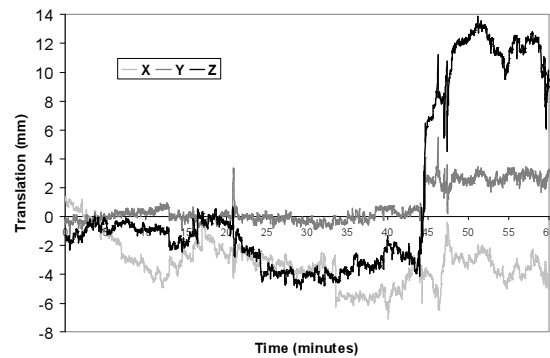


Fig 1 Amount of displacement calculated for the striatal region with respect to its position during the transmission scan experienced by S3 during the scan.

D. ROI placement and ROI based analysis

An HRRT image contains 207 axial planes. ROI placement on so many planes was found to be practically difficult. As a consequence ROIs were placed on regrouped planes obtained by averaging three adjacent axial planes (obtaining an effective plane thickness of 3.6mm). Four circular 47.5mm^2 striatal ROIs were placed on each side of the striatum on three of the regrouped planes (equivalent to 9 original planes) and a cerebellar 2520mm^2 ROI was placed on two regrouped planes to delineate the reference region. TACs were calculated for each ROI and were used as input to the ROI based analysis. The BP obtained from the ROI analysis will be denoted as BP_{ROI} .

E. Parametric analysis

The same cerebellar input function used for the ROI based analysis was used in the voxel based calculation. The parametric images were calculated for the entire volume. In order to compare the parametrically obtained BP values to those obtained with the ROI based approach, three adjacent planes of the parametric images were averaged and the same

ROIs as above were used to delineate the regions across which the parametrically calculated BPs were averaged. The BP obtained from the parametric analysis will be denoted as BP_{par} .

F. Comparison metrics

The following comparisons were performed: (i) BP_{par} vs BP_{ROI} for each method for the realigned and not realigned images; in terms mean values, bias, defined as $(BP_{par} - BP_{ROI})/BP_{ROI}$, and correlation across all ROIs for each subject and (ii) BP_{RTM} vs BP_L for the ROI based and for the parametric approach for the realigned and non realigned data.

III. RESULTS

An example of parametric images obtained with the L method is shown in fig. 2. These images were obtained for S1 where there was only minimal motion.

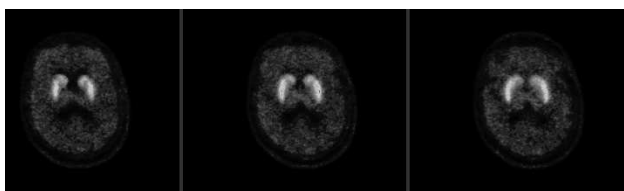


Fig 2. Three regrouped planes showing parametric BP_L values.

A. Comparison between BP_{par} and BP_{ROI}

The BP mean values for each subject calculated for each case are shown in fig. 3 and the bias is shown in fig 4.

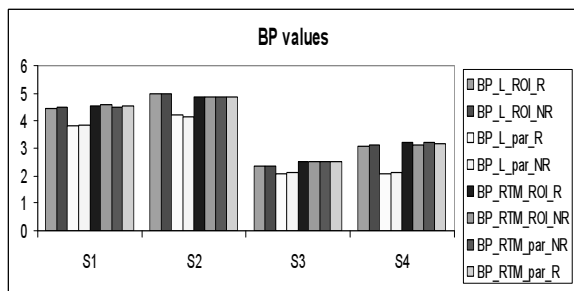


Fig. 3. BP values obtained for each subject with each method: R realigned data, NR non realigned data.

No bias is observed for the RTM approach, while significant bias is observed for the L approach (up to 28%). The bias is present also for the two subjects where minimal motion was observed indicating that the statistical quality of the data is a very important factor in determining the magnitude of the bias associated with the Logan graphical approach. The largest bias was observed for S3, who experienced a lot of motion, in spite of the relatively low BP value, thus emphasizing the compound effect of motion on the bias.

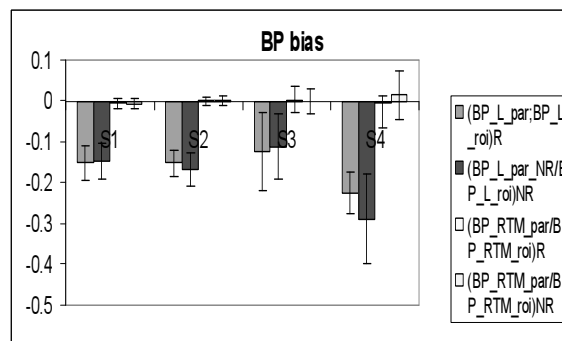


Fig. 4. Bias in the BP values introduced by the parametric approach in fractional values (0 = no bias).

The correlation between BP_{par} and BP_{ROI} is shown in fig. 5.

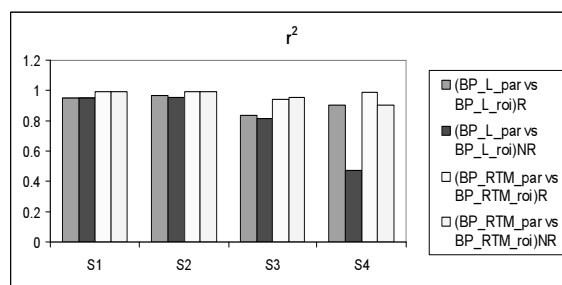


Fig 5. Correlation coefficients between BP_{par} and BP_{ROI} .

The correlation appears always better for the RTM approach ($r^2 > 0.9$) compared to the L approach. Motion has been found to have a negligible effect on the correlation for the RTM approach, while it does affect the L approach (for example, for S4 the correlation goes from $r^2 = 0.5$ in the R case to $r^2 = 0.9$ for the NR case). An example of regression plots for the L method is shown in fig. 6.

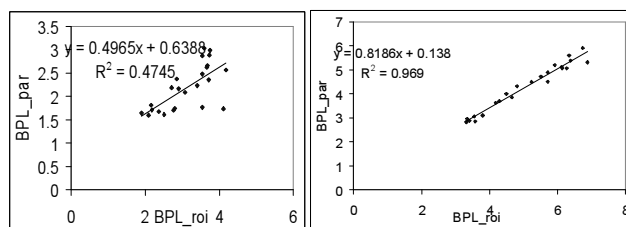


Fig. 6 Example of regression plots between $BP_{L_{par}}$ and $BP_{L_{roi}}$; left S4 NR, significant motion, right S2 R, minimal motion.

B. Comparison between BP_{RTM} and BP_L

The results of the correlation are summarized in table 1. It can be observed that for the two patients that experienced minimal motion (S1 and S2) there is very good correlation between the BP_{RTM} and BP_L regardless of the analysis approach or realignment ($r^2 > 0.94$). For the two subjects that experienced significant motion the correlation between the two methods is significantly worse (r^2 as low as 0.54). For these two cases the frame realignment does improve the

correlation. An on-line motion correction method would likely have an even greater impact on the quality of the correlation. An example of the regression plots between BP_{RTM} and BP_L for the ROI and parametric approach is shown in fig. 7. It is interesting to point out that the regression equations show intercepts different from zero which implies some degree of bias between the two methods; a detailed investigation of this effect is beyond the scope of this study.

TABLE I
RESULTS OF THE REGRESSION BETWEEN BP_{RTM} AND BP_L FOR THE ROI AND PARAMETRIC APPROACH

	ROI based		Parametric		
	BP_{RTM} vs BP_L		BP_{RTM} vs BP_L		
	Regression eq.	r^2	Regression eq.	r^2	
Re-aligned	S1	$y = 0.911x + 0.453$	0.97	$y = 0.985x + 0.756$	0.94
	S2	$y = 0.902x + 0.385$	0.99	$y = 1.092x + 0.278$	0.98
	S3	$y = 0.713x + 0.823$	0.80	$y = 0.520x + 1.426$	0.62
	S4	$y = 0.919x + 0.369$	0.96	$y = 1.119x + 0.521$	0.88
Non aligned	S1	$y = 0.914x + 0.440$	0.97	$y = 0.986x + 0.755$	0.94
	S2	$y = 0.862x + 0.548$	0.98	$y = 1.120x + 0.222$	0.98
	S3	$y = 0.635x + 1.033$	0.67	$y = 0.527x + 1.421$	0.54
	S4	$y = 0.777x + 0.708$	0.89	$y = 0.882x + 1.234$	0.67

maps without any bias in the BP values; the correlation between the BP values obtained with the ROI and the parametric approach is largely independent of subject motion. On the other hand the tissue input Logan approach introduces a noticeable bias in the BP values even in the presence of minimal subject motion. This indicates that the statistical quality of the pixel based data is sufficiently low to make the bias noticeable; thus even in the presence of an accurate on-line motion correction method some degree of bias will be present. Motion also worsens the correlation coefficients between the BP values obtained with the ROI and parametric approach. Approaches where slice regrouping or pixel smoothing before calculating the BP is performed, could be explored as a compromise between accuracy and spatial detail. The amount of bias also depends on the magnitude of the BP values; for RAC the BP values calculated from the data obtained with this scanner range approximately between 2 and 6. For a tracer with lower BP values, the amount of bias will likely be smaller for an equivalent statistical quality of the data and amount of patient motion. The relation between the BP values obtained with the two modeling approaches was found to be noticeably affected by subject motion, indicating that the two methods experience different sensitivities to noise. This is an expected finding, since the two methods use the time information provided by the TACs differently. For the Logan method the early TAC time points contribute to eq. 1 under integration while only the later time points are used as individual values (time points after t , where t is typically 20 min – see methods). In the RTM method all the time points of the TAC are used individually to determine the parameters. The effect of motion must thus be taken into consideration when comparing results obtained with the two methods.

In conclusion, this study shows that parametric imaging with the data acquired on a high resolution PET scanner using standard radioactivity injection amounts is feasible for selected modeling approaches. It also shows that, while similar when calculated on an ROI bases, BP values obtained from different approaches might not relate as well when calculated on a parametric basis. Likewise patient motion further degrades the correlation between the BP values obtained with different approaches; an on-line motion correction will likely make such correlation more robust.

ACKNOWLEDGMENT

The authors thank the UBC/TRIUMF PET group for patient scanning and help with data processing.

REFERENCES

- [1] Logan J, Fowler JS, Volkow ND et al., Distribution volume ratios without blood sampling from graphical analysis of PET data. *J Cereb Blood Flow Metab* 1996;16: 834-840
- [2] Gunn RN, Lammertsma AA, Hume SP, Cunningham VJ. Parametric imaging of ligand-receptor binding in PET using a simplified reference region model. *Neuroimage* 1997 6(4):279-87.

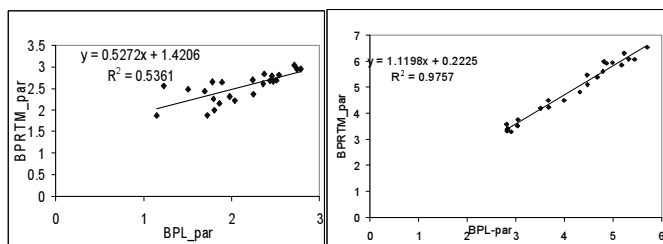


Fig. 7. Example of regression plots between BP_{RTM_par} and BP_{L_par} ; left S3 NR, significant motion, right S2 NR, minimal motion

IV. DISCUSSION AND CONCLUSION

The feasibility of obtaining parametric maps on images generated by the HRRT was tested for two modeling approaches, the RTM and the Logan tissue input method. It was found that the RTM method produces parametric BP

- [3] Lammertsma AA, Hume SP. Simplified reference tissue model for PET receptor studies. *Neuroimage* 1996 4(3):153-8.
- [4] Slifstein M, Laruelle M. Effects of statistical noise on graphic analysis of PET neuroreceptor studies. *J Nucl Med.* 2000 41(12):2083-8.
- [5] Sossi V, de Jong H et al., The second generation HRRT – a multi-centre scanner performance investigation IEEE Nucl Sci Symp Conf Rec 2005 2195-2199
- [6] Polaris, Northern Digital Inc., Waterloo, ON, Canada
- [7] K. Dinelle, S. Blinder, et al Investigation of Subject Motion Encountered During a Typical Positron Emission Tomography Scan Proceedings of the 2006 IEEE/MIC
- [8] D. G. Politte and D. L. Snyder, Corrections for Accidental Coincidences and Attenuation in Maximum-Likelihood Image Reconstruction for Positron-Emission Tomography, *IEEE Trans. Med. Imag.* 1991 10 (1) 82-89